Unspecific peroxygenase enabled formation of azoxy compounds

Li, Huanhuan; Huang, Yawen; Chen, Fuqiang; Zeng, Zhigang; Hollmann, Frank; Wu, Xin; Duan, Peigao; Sheng, Xiang; Zhang, Wuyuan; More Authors

DOI
10.1038/s41467-024-52648-0

Publication date
2024

Document Version
Final published version

Published in
Nature Communications

nature communications

Article

https://doi.org/10.1038/s41467-024-52648-0

Unspecific peroxygenase enabled formation of azoxy compounds

Received: 30 March 2024

Accepted: 17 September 2024

Published online: 27 September 2024

Check for updates

Huanhuan Li[1,2], Yawen Huang[1], Fuqiang Chen[1], Zhigang Zeng[3], Frank Hollmann[4], Xin Wu[1], Xiyang Zhang[1], Peigao Duan[2] ✉, Hao Su[1], Jianjun Shi[5], Xiang Sheng[1] ✉ & Wuyuan Zhang[1] ✉

Enzymes are making a significant impact on chemical synthesis. However, the range of chemical products achievable through biocatalysis is still limited compared to the vast array of products possible with organic synthesis. For instance, azoxy products have rarely been synthesized using enzyme catalysts. In this study, we discovered that fungal unspecific peroxygenases are promising catalysts for synthesizing azoxy products from simple aniline starting materials. The catalytic features (up to 48,450 turnovers and a turnover frequency of 6.7 s^{-1}) and substrate transformations (up to 99% conversion with 98% chemoselectivity) highlight the synthetic potential. We propose a mechanism where peroxygenase-derived hydroxylamine and nitroso compounds spontaneously (non-enzymatically) form the desired azoxy products. This work expands the reactivity repertoire of biocatalytic transformations in the underexplored field of azoxy compound formation reactions.

Functional groups containing a nitrogen-nitrogen bond (e.g., N-N or N = N) are commonly encountered in natural products[1,2]. The reactivity and structural diversity of these molecules are of significant interest in synthetic chemistry. Despite the identification of various compounds with nitrogen-nitrogen bonds in a variety of natural sources, enzymes catalyzing nitrogen-nitrogen bond formation are still underexplored[3–7]. Among these, compounds containing an azoxy group (N = N → O) have been isolated from different taxa, including plants, fungi, and sponges[6,8–12] exhibiting a wide range of biological activities such as antimicrobial and cytotoxic effects[8]. Therefore, it is not very astonishing that modern organic chemistry also focusses on providing synthetic access to a wide range of these important products[13,14]. Azoxy compounds can be synthesized via redox reactions using nitro- or amine-substrates. However, the traditional synthetic methods, such as reductive dimerization of nitrosobenzenes or oxidation of anilines (Fig. 1a), suffer from drawbacks including reliance on hazardous catalysts, poor selectivity and high environmental impact, which are increasingly undesirable in today's chemical industry[15].

Today, only a few enzymes have been reported to catalyze azoxy compound formation reactions (Fig. 1b), limiting their use in organic synthesis. Interestingly, reductive activation of nitro precursors appears to be the preferred synthetic strategy. Nicotinamide cofactor-dependent nitroreductases for example reduce nitrobenzene substrates, often yielding incomplete reductions and a mixture of reaction intermediates[16]. A notable work by Poelarends and coworkers demonstrated a nitroreductase/H_2O_2 system to convert nitrobenzenes into the corresponding azoxy derivates[17]. Recently, an oxidative azoxy-group formation step was proposed in the biosynthesis of azoxymycin and *O*-akylazoxymycins[5,18]. The key enzyme (AzoC) was identified as a nonheme diiron monooxygenase (Fig. 1b). A similar oxygenase (VlmB homologes) was reported for participation in the biosynthesis of valanimycin via a cascade reaction (Supplementary Fig. 1)[6,7]. However, study on AzoC and VlmB homologes are primarily of an enzymological and biochemical nature, focusing on elucidating biosynthetic pathways and enzyme mechanisms.

[1]Key Laboratory of Engineering Biology for Low-carbon Manufacturing, Tianjin Institute of Industrial Biotechnology, Chinese Academy of Sciences, 32 West 7th Avenue, Tianjin 300308, China. [2]School of Chemical Engineering and Technology, Xi'an Jiaotong University, Xi'an 710049, China. [3]School of Nuclear Technology and Chemistry & Biology, Hubei University of Science and Technology, Xianning, Hubei 437100, China. [4]Department of Biotechnology, Delft University of Technology, Vander Maasweg9, 2629 HZ Delft, The Netherlands. [5]College of Chemistry and Chemical Engineering Hainan Normal University Haikou, 571158 Haikou, China. ✉e-mail: pgduan@xjtu.edu.cn; shengx@tib.cas.cn; zhangwy@tib.cas.cn

Fascinated by these reactions, we wondered if peroxygenases would offer a simpler, more robust and efficient, and most importantly, a scalable access to azoxy compounds from simple amine precursors (Fig. 1c). Over the past decade, unspecific peroxygenases (UPOs, EC 1.11.2.1) have emerged as promising biocatalysts for a wide array of challenging reactions, including selective C-H bond oxyfunctionalization, epoxidation, and heteroatom oxidation (*N*- or *S*-oxygenation)[19–22]. We hypothesize that UPOs may also function as *N*-oxygenases, producing generating hydroxylamine- and nitroso-intermediates for spontaneous N-Nbond formation. This strategy would not only expand the reaction repertoire of naturally occurring heme-dependent enzymes but also augment the available enzyme toolboxes for the persistent challenge of azoxy compound synthesis.

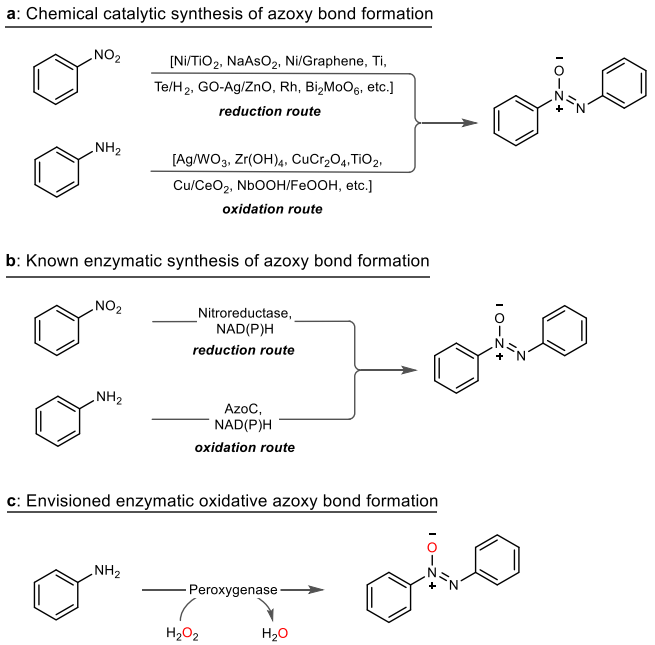

Fig. 1 | Methods for azoxy compound formation reactions. a Chemical methods and (**b**) the so far established biocatalytic methods for azoxy compound synthesis directly using nitro- or amine-substrates. **c** The envisioned enzymatic oxidative azoxy compound synthesis by fungal peroxygenases with simplified electron transport chains.

Results and discussion

Reaction design and characterization

We began with investigating the unspecific peroxygenase from *Agrocybe aegerita* (*Aae*UPO, PaDa-I variant)[23,24] catalyzed transformation of 4-(trifluoromethyl)aniline (**1**, Fig. 2a) and found straightforward conversion into the desired azoxy product. After 8 h, 89.5% of the substrate was converted into the main azoxy product (**1a**, 8.2 mM, 94.5%), along with minor amounts of nitro- (0.6 mM, 1.2%) and azo- (0.5 mM, 4.0%) by-products detected (Fig. 2a). For *Aae*UPO, a total turnover number (TON = $moles_{product} \times moles_{AaeUPO}^{-1}$) of 16900 was determined, aligning well with the generally high catalytic activity of *Aae*UPO and surpassing the performance of most documented synthetic catalysts (Supplementary Table 1). Control experiments confirmed that the reaction proceeded solely in the copresence of *Aae*UPO and H_2O_2. Other heme-containing enzymes such as cytochrome P450 BM3 and horseradish peroxidase (HRP) failed to yield the desired azoxy product (Fig. 2a), highlighting its unique catalytic prowess of *Aae*UPO in facilitating azoxy compound synthesis.

Next, we further characterized the *Aae*UPO-catalyzed conversion of **1** to **1a**. The pH range of the reaction was astonishingly broad with >75% conversion between pH 4 and pH 9. The highest conversion (96.3%) and selectivity (97.3%) were observed at pH 8 (Fig. 2b). The

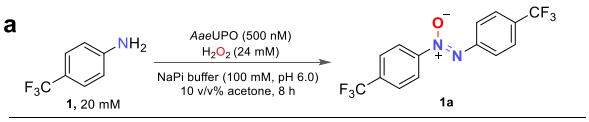

Entry	Variation of the conditions	Conversion (%)	Selectivity of 1 (%)	Selectivity of nitro-& azo-product (%)
1	None	89.5	94.5	5.2
2	No *Aae*UPO	0.6	0	0.6
3	No H_2O_2	0	0	0
4	Thermally inactivated *Aae*UPO	0	0	0
5	P450 with cofactors	0	0	0
6	HRP with H_2O_2	17.0	0	12.8

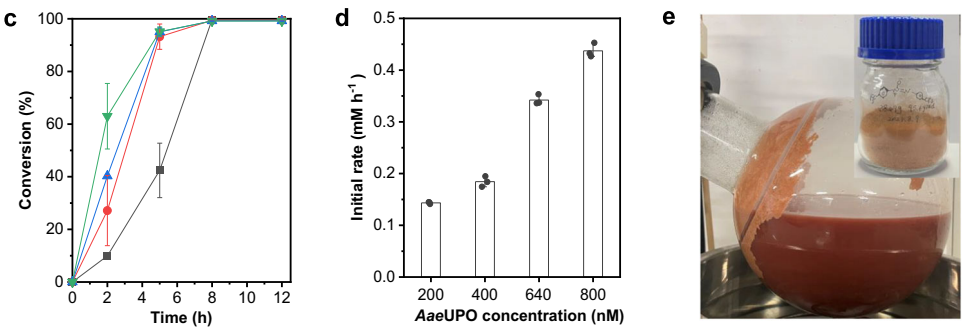

Fig. 2 | Investigation of enzymatic azoxy compound synthesis. Reaction conditions: **a** For P450 and HRP: [**1**] = 2 mM, 30 °C, 10 v/v% acetone, 12 h, 1 mL, [P450 BM3] = 1.46 mg mL^{-1}, [NADPH] = 10 mM, NaPi buffer (100 mM, pH 8.0) or [HRP] = 0.5 mg mL^{-1}, citrate buffer (100 mM, pH 5.0), [H_2O_2] = 1 mM h^{-1}. Reaction conditions unless specifically stated: [**1**] = 20 mM, [*Aae*UPO]= 500 nM, [H_2O_2] = 3 mM h^{-1}, NaPi buffer (100 mM, pH 8.0), 30 °C, 10 v/v% acetone, 8 h, 1 mL. **b** The influence of pH on the product formation: pH = 4 – 9. **c** The influence of H_2O_2 rate: [H_2O_2] = 2 mM h^{-1} (square), 4 mM h^{-1} (circle), 5 mM h^{-1} (triangle), 6 mM h^{-1} (inverted triangle), 12 h. **d** The initial reaction rate at varied *Aae*UPO concentration: [*Aae*UPO] = 200 – 800 nM, 2 h. **e** The setup of a 6 L reaction and the isolated product. Selectivity = [$product_{azoxy}$] / [$products_{in\ total}$] × 100%. The reported value is based on the mean value of triplicate experiments (n = 3).

initial reaction rate depended on both the H_2O_2-addition rate (Fig. 2c) and the *Aae*UPO concentration (Fig. 2d). As the catalytic performance of *Aae*UPO was excellent (turnover frequencies of up to 6.7 s^{-1} and total turnover number of 48,450), the synthetic potential of this reaction was evaluated on 6 L-scale corresponding to a 6000-fold volume increase (Fig. 2e and Supplementary Figs. 2–5). 38.5 g of the desired **1a** were obtained within 11 h reaction time in 95.6% isolated yield. It is interesting to note that during this reaction, no intermediate accumulation of the hydroxylamine product was observable (Supplementary Fig. 5). In view of more sustainable chemistry, we performed an E-factor analysis[25] for the *Aae*UPO-catalyzed azoxy compound synthesis. An E-factor of 170 kg_{waste} $kg_{product}^{-1}$ at first sight does not seem very promising (Supplementary Table 2). Solvents i.e. water (82%), acetone (7.2%) and ethyl acetate (6.9%) accounted for >96% of this E-factor paving the way for more efficient and less environmentally damaging syntheses. We are confident that future optimization such as increasing the reagent loading as well as solvent recycling will drastically reduce the wastes generated. For comparison, we reported a rather low E-factor for enzymatic azoxy-synthesis (Supplementary Table 3), suggesting the great potential of this strategy to access useful organic compounds by biocatalysis.

Substrate and enzyme scope investigations

Having established the *Aae*UPO-catalyzed azoxy compound synthesis reactions, we next explored the product scope of this transformation (Fig. 3 and Supplementary Figs. 6–74). All the 25 aniline derivates tested were transformed in good to excellent conversion with chemoselectivities >70% (generally >90%). Interestingly enough, Hofrichter and coworkers reported predominant ring hydroxylation followed by *Aae*UPO-initiated polymerization under comparable reaction conditions[26]. Our experiments, however, showed a clear preference for azoxy compound formation probably due to the pattern of the ring substitution. The arene substitution pattern had little influence on the outcome of the azoxy compound formation and a broad range of electron-donating and -withdrawing substituents were effectively converted. It is worth noting that in case of alkyl-substituted anilines, trace C-H hydroxylation was observed (Supplementary Table 4), especially the benzylic hydroxylation is well-documented for *Aae*UPO[27]. Apparently, *N*-oxidation is highly favored in our findings.

Next to aniline derivates aminopyridine and aminoquinoline derivatives were also smoothly converted, with chemoselectivities ranging from 70% to 98%. Thermodynamically, trans-configured azoxy compounds should be the favored products. This was confirmed in case of **1a, 18a, 19a, 20a** and **22a**, which were synthesized in semi-preparative quantities, crystallized, and had their crystal structures solved (Fig. 3 and Supplementary Tables 5–9). Hetero-coupling reactions principally are possible as well. The absolute configuration of each asymmetric azoxy compound was assigned by either the corresponding chemical standard or crystal structure (Supplementary Tables 10). However, starting with two different aniline derivatives resulted in a statistical mixture of the four conceivable homo- and hetero-coupling products (Fig. 3, **26a**–**31a** and Supplementary Figs. 75–91). The low selectivity is consistent with the reductive azoxy compound formation[28]. Additionally, we also tested aliphatic amine substrates including cyclopentylamine, n-butylamine, nonylamine and benzylamine, which, however, did not show any desired azoxy products formation with the copresence of *Aae*UPO and H_2O_2.

Other unspecific peroxygenases were also investigated. It was shown that Grogu, *Cci*UPO, *Pab*UPO-II and *Cfu*CPO enabled the conversion of anilines to the corresponding azoxy-aromatic products in satisfactory conversion and selectivity (Supplementary Fig. 92), with TONs up to 50,710. The high catalytic turnover numbers and the varied source of microorganisms of the investigated UPOs suggest the potential of incorporating peroxygenases into natural or engineered metabolic pathways for the biosynthesis of azoxy bond containing compounds[29].

Mechanistic investigation

To gain mechanistic insights into the discovered azoxy bond formation by *Aae*UPO, molecular dynamics (MD) simulations and quantum chemical (QC) calculations were conducted using 4-aminobenzotrifluoride ($ArNH_2$) as a representative substrate. The key steps in the azoxy formation reactions involve the formation of aromatic hydroxylamine (ArNHOH) and nitroso (ArNO) intermediates (Supplementary Fig. 93). In these processes, *Aae*UPO first undergoes activation by H_2O_2, leading to the conversion of iron porphyrin from compound 0 (Cpd 0) to compound I (Cpd I). The mechanism of this activation process has been well-established in previous studies[30–32]. Therefore, MD simulations were performed on the systems where *Aae*UPO is complexed with $ArNH_2$ and ArNHOH, respectively, in the presence of Cpd I (Fig. 4a, b). These enzyme-substrate (ES) complex structures show that the aromatic ring of substrates ($ArNH_2$, ArNHOH) engages in π-π stacking interactions with surrounding residues such as F69, F188 and F191. The -NH_2 and -OH groups form hydrogen bonds with the Cpd I in the corresponding ES structure. Moreover, these groups and Cpd I are also engaged in a hydrogen bond network involving water molecules, R189 and E196.

For the conversion of aniline, two possible mechanisms, the *N*-oxidation mechanism and the hydrogen atom transfer (HAT) mechanism were considered because of the previous proposals for similar reactions by cytochrome P450 monooxygenases[33–35]. The performed computational analysis reveals its adherence to the *N*-oxidation mechanism (Fig. 5a), in which the oxidation is initiated by the rate-determining direct attack of Fe=O center at the amino group with a barrier of 16.1 kcal mol^{-1}. Subsequently, the hydroxylamine is formed by an intramolecular proton transfer via two water molecules (Supplementary Figs. 94–95). In comparison, the barrier of HAT mechanism is slightly higher than the *N*-oxidation mechanism (by 1.4 kcal mol^{-1}, Supplementary Figs. 96–97).

Through two HAT processes, the hydroxylamine is further oxidized to the nitroso product (ArNO) by *Aae*UPO (Fig. 5b). The first HAT is preferred to take place on the hydroxyl group of the hydroxylamine intermediate, leading to the barrier-less formation of a transient oxygen radical (Supplementary Figs. 98–99). The second HAT occurs with a barrier of 3.3 kcal mol^{-1}, where the hydrogen from the -NH group is transferred to Fe-OH, resulting in the formation of ArNO along with the generation of one water molecule. As such, the calculations predicted that the conversion of ArNHOH to ArNO is rapid. This can be corroborated by the experimental observation that ArNHOH was not accumulated in the reaction course (Supplementary Figs. 100–101). Other considered pathways with higher energies for this conversion are given in Supplementary Figs. 89–90. Once the ArNHOH and ArNO intermediates are formed, they can undergo spontaneously chemical dehydration condensation in solution to generate azoxybenzene with a calculated barrier of 15.7 kcal mol^{-1} (Fig. 5c, see also Supplementary Fig. 102 for optimized structures).

For the formation of the azoxy compound, QC results indicate that the ArNHOH and ArNO intermediates can readily condense to generate the azoxy product in solution. First, the -N=O group of ArNO undergoes a nucleophilic attack by ArNHOH, concerted with a proton transfer from the -NH group of ArNHOH to the -N=O group of ArNO, mediated by a water molecule. This results in the formation of an N-N bond between ArNHOH and ArNO. Subsequently, the intermediate formed in the first step is dehydrated to form the azoxy compound. The calculated energy barrier for the entire process is 15.7 kcal mol^{-1}. Moreover, the reaction is significantly exothermic, with the energy of the azoxy product being lower than that of the reactants by

https://doi.org/10.1038/s41467-024-52648-0

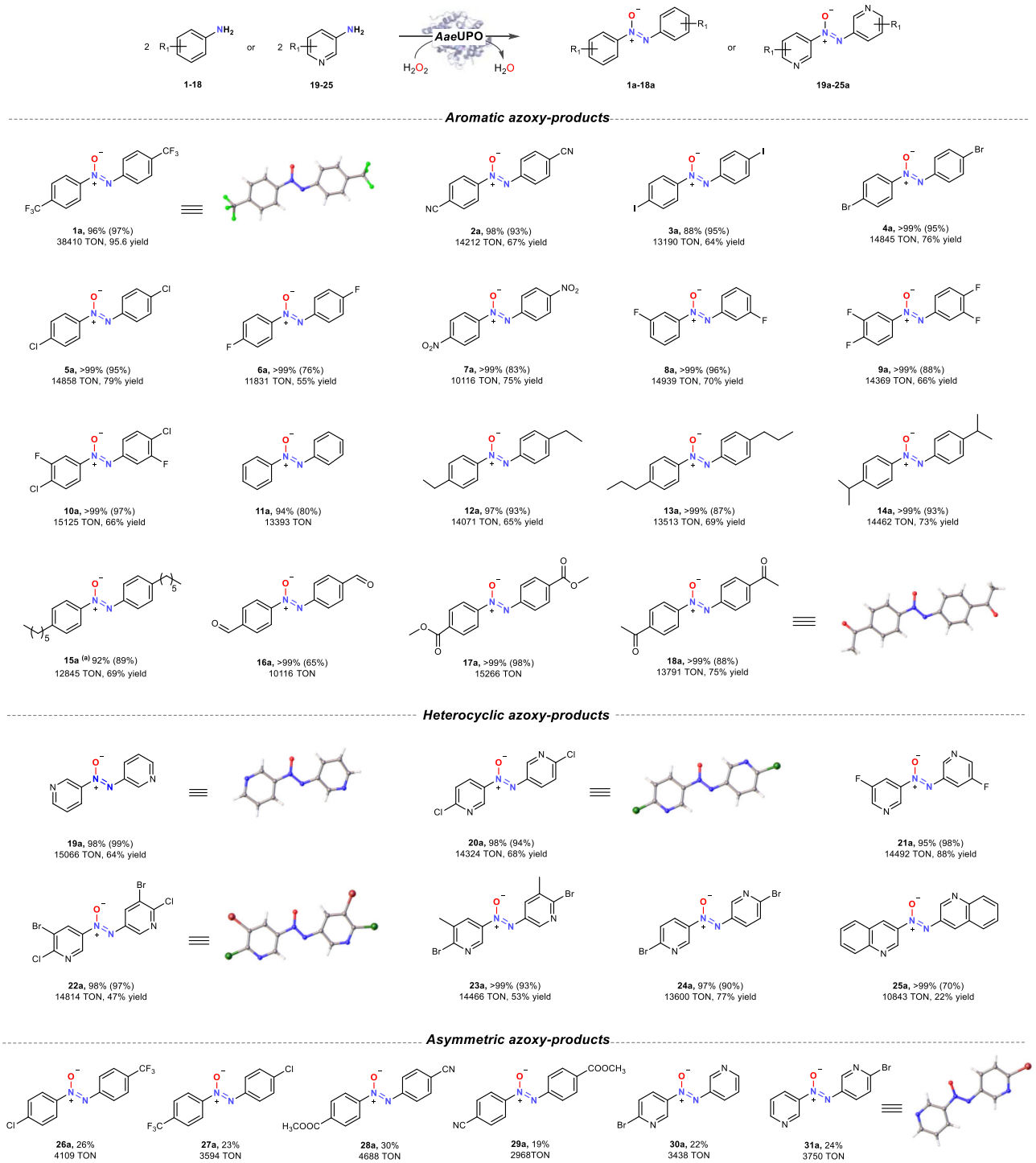

Fig. 3 | Substrate scope of *Aae*UPO-catalyzed azoxy compound synthesis. The substituted anilines using the following conditions: [substrate] = 20 mM, [*Aae*UPO] = 640 nM, [H_2O_2] = 4 mM h^{-1}, NaPi buffer (100 mM, pH 8.0), 30 °C, 10 v/v % acetone, 12 h, 1 mL. TON = [**1a** –**31a**] / [*Aae*UPO]. The conversion was based on the area estimation. The yield was calculated from the amount of isolated product in a 50 mL scale, except for **1a** in a 6 L, with selectivity indicated in parentheses. [a] The reaction time was 20 h. Duplicate experiments were performed ($n = 2$).

31.1 kcal mol^{-1}. Thus, the condensation between ArNHOH and ArNO in solution is both kinetically feasible and thermodynamically favorable.

Although the *Aae*UPO-catalyzed azoxy compound synthesis showed predominant chemoselectivity, the studies on the observed minor nitro- and azo-products are valuable to decipher the differences between *Aae*UPO and the P450 monooxygenases. In the case of azobenzene formation by *Aae*UPO, QC calculations indicate that it is a process with a high energy barrier (26.6 kcal mol^{-1}), consistent with the experimental observation (Supplementary Fig. 105). As for the nitro product, its formation is speculated through the direct oxidation of ArNO by Cpd I. However, MD simulations of *Aae*UPO complexed with ArNO revealed that ArNO is not preferred to bind in the active site (Supplementary Fig. 106). To assess the chemical feasibility of this oxidation, QC calculations using a simplified model comprising only Cpd I and ArNO were performed. It was shown that Cpd I can readily oxidize ArNO to $ArNO_2$ with a barrier of 10.5 kcal mol^{-1}, suggesting that

https://doi.org/10.1038/s41467-024-52648-0

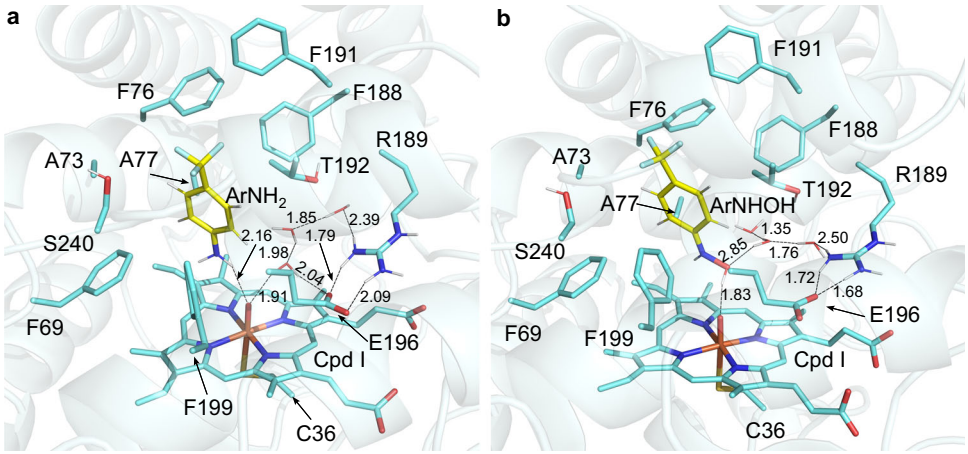

Fig. 4 | The interactions between the substrate and active site residues. Representative conformations from MD simulations for the enzyme in complex with $ArNH_2$ (**a**) and ArNHOH (**b**) in the presence of Cpd I. For clarity, most of the non-polar hydrogen atoms are omitted. Key distances are shown in angstroms.

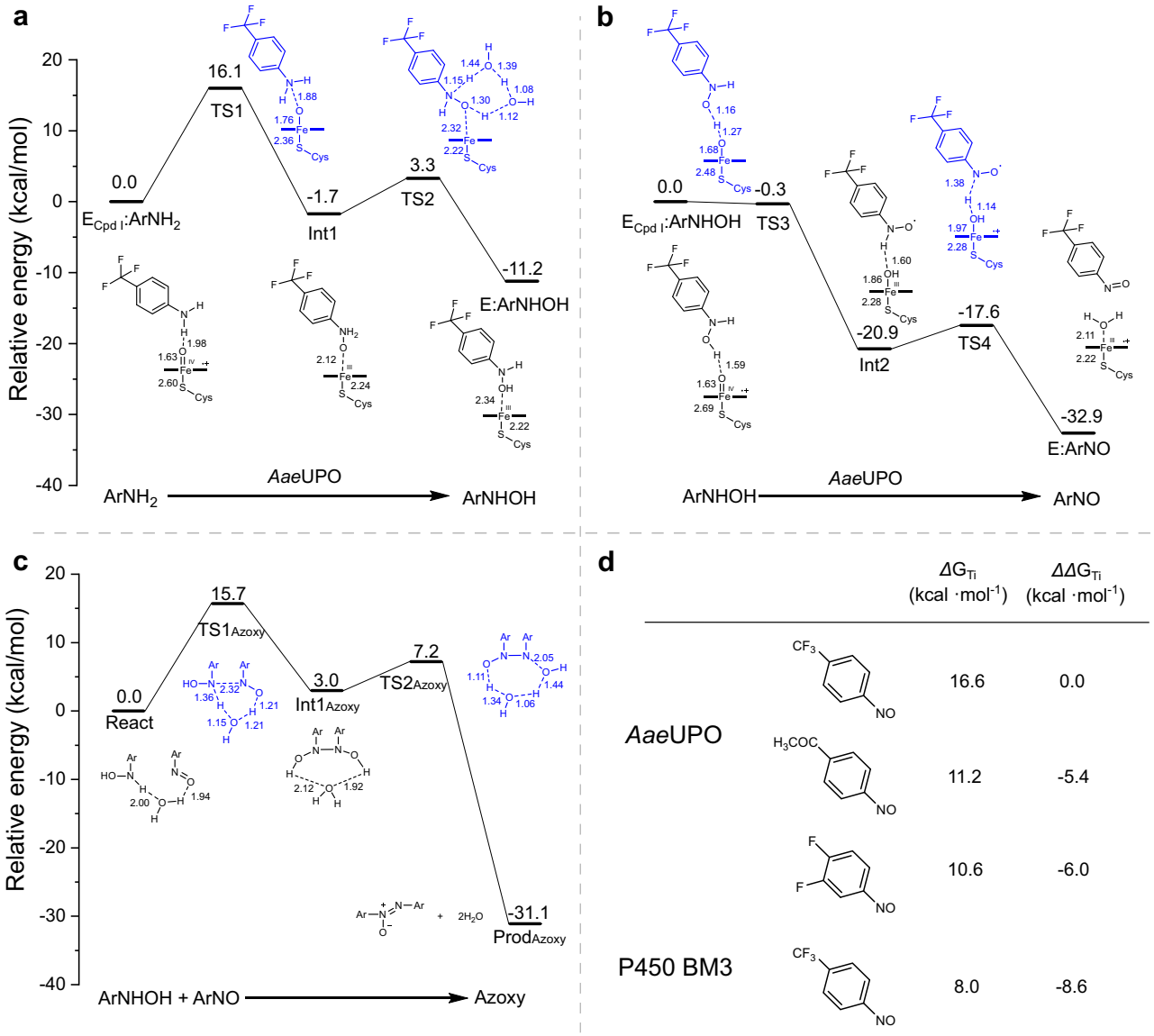

Fig. 5 | Mechanistic study of the *Aae*UPO-catalyzed azoxy compound synthesis from aniline. The energy profiles for the catalytic oxidation of $ArNH_2$ to ArNHOH (**a**), the subsequent oxidation of ArNHOH to ArNO (**b**), the formation of azoxybenzene from ArNHOH and ArNO in water solution (**c**), as well as the relative binding energies of anilines in *Aae*UPO and P450 BM3 enzymes (**d**). The optimized full structures and spin densities are provided in supplementary materials.

the difficulties in forming $ArNO_2$ indeed stem from the unfavorable binding of ArNO to *Aae*UPO (Supplementary Fig. 107). This is further supported by the much higher binding free energy of ArNO compared to $ArNH_2$, by ca 16.6 kcal mol^{-1} obtained by using thermodynamic integration (Ti) method (Fig. 5d)[36]. Experimentally, substituting aniline using 4-$COCH_3$ or 3,4-F instead of 4-CF_3 resulted in increased ratios of the nitro products. Indeed, the binding of these two nitroso compounds are favorable than ArNO characterized by lower relative binding energies (Fig. 5d). This explanation can also be applied to the inability of P450 BM3 to promote the azoxy bond construction. The binding energy of ArNO, compared to $ArNH_2$, is 8.6 kcal mol^{-1} lower in P450 BM3 than in *Aae*UPO (Fig. 5d). This shows that ArNO has a higher affinity for the protein pocket of P450 BM3, making it more readily further oxidized to $ArNO_2$ by P450 BM3 than by *Aae*UPO.

In summary, chemical transformations using enzymes represent a frontier in modern chemistry. While protein engineering has proven to be a powerful approach in creating catalysts to expand the boundaries of chemistry, there is still large space to explore the unknown functions of natural enzymes. The latter holds great promise in expanding the reactivity repertoire of the natural biocatalysts[37]. The envisioned azoxy compound synthesis reaction demonstrates the potential of unspecific peroxygenases as robust catalysts to achieve synthetic reactivities that have not realized by other heme enzymes. Fungal unspecific peroxygenases, a family of heme-dependent enzymes, may be particularly useful to enable efficient and sustainable functionalization of simple anilines to produce valuable azoxy containing chemicals. Furthermore, apart from the enzymatic methodology, the ability to construct diverse functional azoxy bonds can expand their application in agrochemicals, pharmaceuticals, pigments, and liquid crystals. Finally, the obtained structural and energetic insights not only provide valuable understanding of *Aae*UPO-catalyzed reactions but also offer guidance for the rational design of heme-dependent UPO and P450 BM3 with tailored activity. Notably, the calculations revealed that the less favorable binding of the nitroso-intermediate in *Aae*UPO, compared to P450 BM3, promotes more efficient synthesis of azoxy compounds over nitro-products. This finding can inform the strategic design of P450 BM3 mutants aimed at modifying product preference.

Methods

General procedures for the enzymatic azoxy compound synthesis

In a 2 mL transparent glass vial, 20 mM of the amine substrate (**1**) and 640 nM of *Aae*UPO (crude extract, Supplementary Figs. 110–111) were added to NaPi buffer (100 mM, pH 8) with 10 v/v% acetone. The reaction volume was adjusted to 1 mL after adding all reaction components. Afterwards, the H_2O_2 from an 800 mM stock solution was supplied by a syringe pump at a rate of 4.98 μL h^{-1}, corresponding to a concentration of 4 mM h^{-1}. The reaction vial was agitated in a thermal shaker at 800 rpm and 30 °C. During the reaction course, 100 μL of the reaction mixture was withdrawn and extracted with 200 μL of ethyl acetate (extraction ratio: 1:2) containing the inner standard (dodecane). After mixing and separation by centrifugation (10,000 × g, 1 min), the organic layer of ethyl acetate was dried over anhydrous Na_2SO_4 before analysis by GC or GC-MS. To quantify the conversion of the aniline into the azoxy product, calibration curves were used for the model reaction (Supplementary Figs. 112–114), whereas the other substrates were quantified by the peak area. Triplicate experiments were performed and three independent data were used for analysis. To investigated the substrate scope, in a 100 mL glass bottle, 40 mM of aniline substrate and 640 nM of *Aae*UPO (crude extract) were added to NaPi buffer (100 mM, pH 8.0) with 10 v/v% acetone. The reaction volume was adjusted to 50 mL using the same buffer. Then, H_2O_2 from an 800 mM solution was dosed by a syringe pump at a rate of 250 μL h^{-1}, corresponding to a concentration of 4 mM h^{-1}. The reaction was stirred at 400 rpms and 30 °C. Upon the completion of the reaction monitored by thin-layer chromatography, the mixture was extracted with 50 mL of ethyl acetate three times and dried over Na_2SO_4. The solvent was evaporated at 40 °C under reduced pressure. The target compounds were purified by flash chromatography (Biotage rapid preparation system) using 0–35% ethyl acetate in petroleum ether. The targeting compounds were analyzed by ^1H NMR, ^{13}C NMR and GC-MS. The isolated yields were calculated based on the actual amount of azoxy products compared to the theoretical yield.

Computational study

To gain mechanistic insights into the *Aae*UPO-catalyzed oxidation of anilines, molecular dynamics (MD) simulations and quantum chemical (QC) calculations were performed using the computational models designed on the basis of the previously solved crystal structure (PDB ID: 6EKZ)[38]. Details of the computational methods and the technical aspects are provided in the Supplementary Information. The optimized geometries and the energy profiles calculated by QC are shown in Supplementary Figs. 94–99, 103–105 and 107, and the spin densities of the optimized intermediates and transition states are summarized in Supplementary Tables 11–12. The root mean square deviation (RMSD) and distance analysis of the MD simulations are shown in Supplementary Figs. 106 and 108–109.

Reporting summary

Further information on research design is available in the Nature Portfolio Reporting Summary linked to this article.

Data availability

All data are available in the main text or the supplementary information file. Crystallographic data for the structures reported in this article have been deposited at the Cambridge Crystallographic Data Centre, under deposition numbers 2303483 (**1a**), 2303495 (**18a**), 2303477 (**19a**), 2303494 (**20a**), 2303524 (**22a**) and 2376593 (**31a**). Copies of the data can be obtained free of charge via https://www.ccdc.cam.ac.uk/structures/. Source data are provided with this paper. All data are available from the corresponding author upon request. Source data are provided with this paper.

References

1. Waldman, A. J., Ng, T. L., Wang, P. & Balskus, E. P. Heteroatom - heteroatom bond formation in natural product biosynthesis. *Chem. Rev.* **117**, 5784–5863 (2017).
2. Katsuyama, Y. & Matsuda, K. Recent advance in the biosynthesis of nitrogen - nitrogen bond containing natural products. *Curr. Opin. Chem. Biol.* **59**, 62–68 (2020).
3. Sugai, Y., Katsuyama, Y. & Ohnishi, Y. A nitrous acid biosynthetic pathway for diazo group formation in bacteria. *Nat. Chem. Biol.* **12**, 73–75 (2016).
4. Du, Y.-L., He, H.-Y., Higgins, M. A. & Ryan, K. S. A heme-dependent enzyme forms the nitrogen-nitrogen bond in piperazate. *Nat. Chem. Biol.* **13**, 836–838 (2017).
5. Guo, Y.-Y. et al. Molecular mechanism of azoxy bond formation for azoxymycins biosynthesis. *Nat. Commun.* **10**, 4420 (2019).
6. Zheng, Z. et al. Reconstitution of the final steps in the biosynthesis of valanimycin reveals the origin of its characteristic azoxy moiety. *Angew. Chem. Int. Ed.* **63**, e202315844 (2024).
7. Shi, J. et al. Conserved enzymatic cascade for bacterial azoxy biosynthesis. *J. Am. Chem. Soc.* **145**, 27131–27139 (2023).
8. Wibowo, M. & Ding, L. Chemistry and biology of natural azoxy compounds. *J. Nat. Prod.* **83**, 3482–3491 (2020).
9. Chen, L., Deng, Z. & Zhao, C. Nitrogen-nitrogen bond formation reactions involved in natural product biosynthesis. *ACS Chem. Biol.* **16**, 559–570 (2021).
10. Manderscheid, N. et al. Elaiomycins K and L, new azoxy antibiotics from *Streptomyces sp.* Tü 6399. *J. Antibiot.* **66**, 85–88 (2013).

11. He, X. et al. O-alkylazoxymycins A-F, naturally occurring azoxy-aromatic compounds from Streptomyces sp. Py50. *J. Nat. Prod.* **86**, 176–181 (2023).
12. Maleckis, M. et al. Biosynthesis of the azoxy compound azodyrecin from Streptomyces mirabilis P8-A2. *ACS Chem. Biol.* **19**, 641–653 (2024).
13. Cai, B.-G., Empel, C., Yao, W. Z., Koenigs, R. M. & Xuan, J. Azoxy compounds- from synthesis to reagents for azoxy group transfer reactions. *Angew. Chem. Int. Ed.* **62**, e202312031 (2023).
14. Li, Z. et al. Solvent-free selective hydrogenation of nitroaromatics to azoxy compounds over Co single atoms decorated on Nb_2O_5 nanomeshes. *Nat. Commun.* **15**, 3195 (2024).
15. Grirrane, A., Corma, A. & García, H. Gold-catalyzed synthesis of aromatic azo compounds from anilines and nitroaromatics. *Science* **322**, 1661–1664 (2008).
16. Pitsawong, W., Hoben, J. P. & Miller, A.-F. Understanding the broad substrate repertoire of nitroreductase based on its kinetic mechanism. *J. Biol. Chem.* **289**, 15203–15214 (2014).
17. Luján, A. P. et al. Tailored photoenzymatic systems for selective reduction of aliphatic and aromatic nitro compounds fueled by light. *Nat. Commun.* **14**, 5442 (2023).
18. Guo, Y.-Y. et al. Chemoenzymatic synthesis of phenol diarylamine using non-heme diiron N-oxygenase. *ACS Catal.* **13**, 1412–1417 (2023).
19. Sigmund, M.-C. & Poelarends, G. J. Current state and future perspectives of engineered and artificial peroxygenases for the oxyfunctionalization of organic molecules. *Nat. Catal.* **3**, 690–702 (2020).
20. Grogan, G. Hemoprotein catalyzed oxygenations: P450s, UPOs, and progress toward scalable reactions. *JACS Au* **1**, 1312–1329 (2021).
21. Wang, Y. H., Lan, D. M., Durrani, R. & Hollmann, F. Peroxygenases en route to becoming dream catalysts. what are the opportunities and challenges? *Curr. Opin. Chem. Biol.* **37**, 1–9 (2017).
22. Li, H. et al. A simple access to γ- and ε-keto arenes via enzymatic divergent C-H bond oxyfunctionalization. *Adv. Sci.* **10**, e2304605 (2023).
23. Molina Espeja, P., Ma, S., Mate, D. M., Ludwig, R. & Alcalde, M. Tandem-yeast expression system for engineering and producing unspecific peroxygenase. *Enzym. Microb. Tech.* **73**, 29–33 (2015).
24. Ullrich, R., Nüske, J., Scheibner, K., Spantzel, J. & Hofrichter, M. Novel haloperoxidase from the agaric basidiomycete *Agrocybe aegerita* oxidizes aryl alcohols and aldehydes. *Appl. Environ. Microb.* **70**, 4575–4581 (2004).
25. Sheldon, R. A. The E factor at 30: a passion for pollution prevention. *Green. Chem.* **25**, 1704–1728 (2023).
26. Wu, Y. et al. Direct electron transfer of *Agrocybe aegerita* peroxygenase at electrodes modified with chitosan-capped Au nanoparticles and its bioelectrocatalysis to aniline. *Sens. Actuator B: Chem.* **160**, 1419–1426 (2011).
27. Xu, X., Hilberath, T. & Hollmann, F. Selective oxyfunctionalisation reactions catalysed by P450 monooxygenases and peroxygenases-a bright future for sustainable chemical synthesis. *Curr. Opin. Green. Sust. Chem.* **39**, 100745 (2023).
28. Dai, Y. et al. Light-tuned selective photosynthesis of azo- and azoxy-aromatics using graphitic C_3N_4. *Nat. Commun.* **9**, 60 (2018).
29. Van Cura, D. et al. Discovery of the azaserine biosynthetic pathway uncovers a biological route for α-diazoester production. *Angew. Chem. Int. Ed.* **62**, e202304646 (2023).
30. Lai, W., Chen, H., Cho, K. B. & Shaik, S. Effects of substrate, protein environment, and proximal ligand mutation on compound I and compound 0 of chloroperoxidase. *J. Phys. Chem. A* **113**, 11763–11771 (2009).
31. Chen, H., Hirao, H., Derat, E., Schlichting, I. & Shaik, S. Quantum mechanical/molecular mechanical study on the mechanisms of compound I formation in the catalytic cycle of chloroperoxidase: an overview on heme enzymes. *J. Phys. Chem. B* **112**, 9490–9500 (2008).
32. Costa, G. J. & Liang, R. Understanding the multifaceted mechanism of Compound I formation in *Unspecific Peroxygenases* through multiscale simulations. *J. Phys. Chem. B* **127**, 8809–8824 (2023).
33. Ji, L. & Schüürmann, G. Model and mechanism: N-hydroxylation of primary aromatic amines by cytochrome P450. *Angew. Chem. Int. Ed.* **52**, 744–748 (2013).
34. Lonsdale, R., Fort, R. M., Rydberg, P., Harvey, J. N. & Mulholland, A. J. Quantum mechanics/molecular mechanics modeling of drug metabolism: mexiletine N-hydroxylation by cytochrome P450 1A2. *Chem. Res. Toxicol.* **29**, 963–971 (2016).
35. Seger, S. T., Rydberg, P. & Olsen, L. Mechanism of the N-hydroxylation of primary and secondary amines by cytochrome P450. *Chem. Res. Toxicol.* **28**, 597–603 (2015).
36. Kirkwood, J. G. Statistical mechanics of fluid mixtures. *J. Chem. Phys.* **3**, 300–313 (2004).
37. Huang, X. et al. Photoenzymatic enantioselective intermolecular radical hydroalkylation. *Nature* **584**, 69–74 (2020).
38. Ramirez-Escudero, M. et al. Structural insights into the substrate promiscuity of a laboratory-evolved peroxygenase. *ACS Chem. Biol.* **13**, 3259–3268 (2018).

Acknowledgements

We thank Prof. Yanhe Ma for the insightful evaluation on the conceptual and experimental results. We also thank Prof. Weidong Liu, Jie Zhang, Prof. Shaoping Fu and Xuechen Yang and Yonghong Yao for their help in the X-ray crystallography, scaled-up reactions and high-resolution mass. We appreciate the financial support from National Key R&D Program of China (2023YFC3403600), National Natural Science Foundation of China (No. 32171253), and Tianjin Synthetic Biotechnology Innovation Capacity Improvement Project (No. TSBI-CIP-CXRC-032) received by W.Z. Also, X. S. acknowledges the National Key R&D Program of China (2021YFA0911500) for the financial support.

Author contributions

H.L. developed the enzymatic nitrogen-nitrogen formation system and performed most of the experiments. Y.H., Z.Z., X.Z., X.W. and J.S. assisted the synthetic experiments. F.C., H.S. and X.S. conducted theoretical modeling. P.D. coordinated the project. H.L., F.C., F.H., X.W. and W.Z. cowrote the manuscript, with input from all authors.

Competing interests

The authors declare no competing interests.

Additional information

Supplementary information The online version contains supplementary material available at https://doi.org/10.1038/s41467-024-52648-0.

Correspondence and requests for materials should be addressed to Peigao Duan, Xiang Sheng or Wuyuan Zhang.

Peer review information *Nature Communications* thanks Pedro Alexandrino Fernandes, Yuan-Yang Guo and the other anonymous reviewer(s) for their contribution to the peer review of this work. A peer review file is available.